ARTICLE
Journal of Cellular Biochemistry 113:2432–2441 (2012)

Journal of Cellular Biochemistry

A Novel *Phex* Mutation in a New Mouse Model of Hypophosphatemic Rickets

Celeste Owen,[1] Frieda Chen,[2] Ann M. Flenniken,[1] Lucy R. Osborne,[1,2,3] Shoji Ichikawa,[4] S. Lee Adamson,[1,5,6] Janet Rossant,[1,2,7] and Jane E. Aubin[1,2*]

[1]*Centre For Modeling Human Disease, Samuel Lunenfeld Research Institute, Mount Sinai Hospital, 600 University Avenue, Toronto, Ontario, Canada M5G 1X5*

[2]*Department of Molecular Genetics, University of Toronto, Toronto, Ontario, Canada M5S 1A8*

[3]*Department of Medicine, University of Toronto, Toronto, Ontario, Canada M5S 1A8*

[4]*Department of Medicine, Indiana University School of Medicine, Indianapolis, Indiana*

[5]*Department of Obstetrics and Gynecology, University of Toronto, Toronto, Ontario, Canada M5S 1A8*

[6]*Heart and Stroke/Richard Lewar Centre of Excellence, University of Toronto, Toronto, Ontario, Canada M5S 1A8*

[7]*Program in Developmental and Stem Cell Biology, The Hospital for Sick Children, Toronto, Ontario, Canada M5G 1L7*

ABSTRACT

X-linked hypophosphatemic rickets (XLH) is a dominantly inherited disease characterized by renal phosphate wasting, aberrant vitamin D metabolism, and defective bone mineralization. It is known that XLH in humans and in certain mouse models is caused by inactivating mutations in *PHEX/Phex* (phosphate-regulating gene with homologies to endopeptidases on the X chromosome). By a genome-wide *N*-ethyl-*N*-nitrosourea (ENU)-induced mutagenesis screen in mice, we identified a dominant mouse mutation that exhibits the classic clinical manifestations of XLH, including growth retardation, skeletal abnormalities (rickets/osteomalacia), hypophosphatemia, and increased serum alkaline phosphatase (ALP) levels. Mapping and sequencing revealed that these mice carry a point mutation in exon 14 of the Phex gene that introduces a stop codon at amino acid 496 of the coding sequence ($Phex^{Jrt}$ also published as $Phex^{K496X}$ [Ichikawa et al., 2012]). Fgf23 mRNA expression as well as that of osteocalcin, bone sialoprotein, and matrix extracellular phosphoglycoprotein was upregulated in male mutant long bone, but that of sclerostin was unaffected. Although Phex mRNA is expressed in bone from mutant hemizygous male mice ($Phex^{Jrt}$/Y mice), no Phex protein was detected in immunoblots of femoral bone protein. Stromal cultures from mutant bone marrow were indistinguishable from those of wild-type mice with respect to differentiation and mineralization. The ability of $Phex^{Jrt}$/Y osteoblasts to mineralize and the altered expression levels of matrix proteins compared with the well-studied *Hyp* mice makes it a unique model with which to further explore the clinical manifestations of XLH and its link to FGF23 as well as to evaluate potential new therapeutic strategies. J. Cell. Biochem. 113: 2432–2441, 2012. © 2012 Wiley Periodicals, Inc.

KEY WORDS: *N*-ETHYL-*N*-NITROSOUREA MUTAGENESIS; BONE; MINERALIZATION; ENDOPEPTIDASE

X-linked hypophosphatemic rickets (XLH) is the most common form of inherited rickets in humans, with 1 in 20,000 individuals affected by this phosphate disorder [Sabbagh et al., 2000], and ranges widely in its clinical phenotype from mild isolated incidences of hypophosphatemia to severe osteomalacia [Lobaugh et al., 1984]. It is a dominantly inherited disease characterized by renal phosphate wasting with resulting hypophosphatemia, aberrant vitamin D metabolism, stunted growth, and defective mineralization of bone, cartilage, and teeth [Rasmussen and Tenenhouse, 1995].

The authors declare no conflicts of interest.

Celeste Owen and Frieda Chen contributed equally to this work.

Grant sponsor: Genome Canada and the Ontario Genomic Institute; Grant sponsor: Canadian Institutes of Health Research (Centre for Modeling Human Disease); Grant number: FRN 69198; Grant sponsor: Indiana Clinical and Translational Sciences Institute; Grant sponsor: National Institutes of Health; Grant number: RR025760.

*Correspondence to: Jane E. Aubin, PhD, Faculty of Medicine, Department of Molecular Genetics, University of Toronto, Room 4245 Medical Sciences Building, 1 King's College Circle, Toronto, Ontario, Canada M5S 1A8.
E-mail: jane.aubin@utoronto.ca

Manuscript Received: 22 February 2012; Manuscript Accepted: 24 February 2012

Accepted manuscript online in Wiley Online Library (wileyonlinelibrary.com): 2 March 2012

DOI 10.1002/jcb.24115 • © 2012 Wiley Periodicals, Inc.

Although XLH was first observed and described as vitamin D-resistant rickets over 70 years ago, it was not until the mid-1990s that the *PHEX/Phex* (phosphate-regulating gene with homologies to endopeptidases on the X chromosome) gene was successfully identified [Francis et al., 1995; Du et al., 1996; Holm et al., 1997; Rowe et al., 1997]. *PHEX/Phex* encodes a protein that is a member of the M13 class of cell-surface zinc-dependant proteases. It is comprised of 749 amino acids organized into three domains: a small amino-terminal intracellular tail, a short transmembrane domain, and a large carboxyterminal extracellular domain that contains 10 highly conserved cysteine residues and a zinc-binding motif that in other members of the zinc metallopeptidase family are required for conformation and activity, respectively [Turner and Tanzawa, 1997]. In spite of these conserved structures, no physiological substrate for PHEX has yet been identified.

Over 280 mutant PHEX alleles have been identified in XLH and include duplications, insertions, deletions, missense, and splice site mutations in both coding and non-coding regions of the gene (see PHEXdb http://www.phexdb.mcgill.ca [Sabbagh et al., 2000]). No clear correlation between the type or location of the mutation and the severity of the disease has been found [Francis et al., 1997; Holm et al., 1997; Rowe et al., 1997; Filisetti et al., 1999; Tenenhouse, 1999; Drezner, 2000; Christie et al., 2001; Holm et al., 2001; Sabbagh et al., 2003; Ichikawa et al., 2008]; furthermore, hemizygous males and heterozygous females are similarly affected despite an expected gene dosage effect [Holm et al., 2001]. A large number of mutations occur randomly across mainly the extracellular domain, which is encoded by exons 2–22, but mutational hotspots (e.g., the G nucleotide at 1735) appear to exist [Francis et al., 1997; Rowe et al., 1997; Filisetti et al., 1999] and a mutation in the 3′-UTR has also recently been identified [Ichikawa et al., 2008]. All are thought to lead to loss-of-function, or, in the case of that in the 3′-UTR, impaired protein production.

Many studies are ongoing to address precisely how PHEX loss-of-function leads to the biochemical and skeletal abnormalities observed in XLH (reviewed in [Liu et al., 2007; Strom and Juppner, 2008]) with an evolving picture of the multiple factors, such as fibroblast growth factor 23 (FGF23) involved in a bone–kidney axis regulating phosphate homeostasis and matrix extracellular phosphoglycoprotein (MEPE) involved in disruption of matrix mineralization. Much of this work has involved the use of mouse models of XLH, through which additional information has been gleaned, such as whether osteoblasts from mutant or conditional null *Phex* models have cell autonomous defects and whether they bring about particular features of the XLH phenotype. For example, osteoblasts from *Hyp* mice, which do not express PHEX [Miao et al., 2001], are unable to mineralize in vitro [Xiao et al., 1998]. It has also been shown that a mouse model with an osteoblast-specific knockout of *Phex* can reproduce the increased FGF23 levels, phosphaturia, and osteomalacia typical of XLH [Liu et al., 2002; Yuan et al., 2008].

To date, seven mutations in *Phex* leading to XLH have been identified in mouse, including *Hyp*, *Gy* [Strom et al., 1997], *Ska1* [Carpinelli et al., 2002], *Hyp-Duk*, *Hyp-2J* [Lorenz-Depiereux et al., 2004], *Pug* [Xiong et al., 2008], and *Kbus/Idr* [Moriyama et al., 2011]. Two of these (*Ska1* and *Pug*) have resulted from *N*-ethyl-*N*-nitrosourea (ENU) mutagenesis screens. Here, we report a novel ENU-induced mouse line Phex^{Jrt}, carrying a point mutation in exon 14 of *Phex* that introduces a premature stop codon at amino acid 496 in Phex (K496X). These hemizygous male and heterozygous female Phex^{Jrt} mice exhibit the classic clinical manifestations of XLH, including growth retardation, hypophosphatemia, skeletal abnormalities (rickets/osteomalacia), but a striking lack of an intrinsic osteoblast mineralization defect as well as differences in mRNA expression levels of several matrix proteins make it a valuable addition to existing mouse models in the study of PHEX and its multipath role in mineralization.

MATERIALS AND METHODS

MICE AND ENU MUTAGENESIS

129S1/SVImJ (129) males and C57BL/6J (B6) females were purchased from the Jackson Laboratory (Bar Harbor, ME) at 6–8 weeks of age. Male 129S1/SvImJ mice received two intraperitoneal injections of ENU (Sigma–Aldrich), 7 days apart, at a dose of 100 mg/kg. ENU mutagenized males were allowed 8 weeks to recover fertility, and then were bred to C57BL/6J females. The offspring produced from these matings were 129;B6F1 hybrid pups (G1) that were screened for traits of interest, including abnormalities in bone mineral density (BMD; see below). BMD phenodeviants were bred to C57BL/6J mice, and the G2s (B6;CgN2) produced were tested for heritability of the trait and were subsequently used for genetic mapping. Lines were maintained by backcrossing to C57BL/6J mice. Mice from seven generations on C57BL/6J G7(B6;CgN7) and higher were used in this study. All mice received a diet of standard laboratory chow (Purina Rodent Diet 20 5053). All animal experimental procedures were approved by the local Animal Care Committees at the Samuel Lunenfeld Research Institute and the University of Toronto, and were conducted in accordance with the guidelines of the Canadian Council on Animal Care. Due to the stochastic nature of X-inactivation and the likelihood of greater phenotypic variation in female heterozygotes, male mice were used for the majority of experiments.

GENETIC MAPPING

DNA was extracted from tail tissue using standard procedures followed by PCR amplification of individual microsatellite markers using fluorescently tagged primers (IDT, Coralville, IA). Cycles were performed as follows: 94°C for 3 min, 35 cycles of 94°C for 30 s, 55°C for 30 s, and 72°C for 30 s, and a final extension of 72°C for 5 min. The labeled products were then multiplexed and analyzed on a BaseStation automated sequencer (MJ Research, Waltham, MA) to determine whether, for any given marker, an allele from the mutagenized strain (129S1/SVImJ) had been inherited. The specific mutation was identified by direct sequencing of *Phex* exons from amplified genomic DNA.

BONE MINERAL DENSITY

Dual energy X-ray absorptiometry was performed using a PIXImus small animal densitometer (Lunar; GE Medical System, WI). Mice were anesthetized using 5% isoflurane with 700 ml/min oxygen, and placed in prone position on the specimen tray using 2% isoflurane with 700 ml/min oxygen to maintain anesthesia. Following whole

body scanning, bone mineral content (BMC), bone area, and BMD were measured, with the skull excluded from results. For screening, male and female mice were tested initially at 8 weeks of age, and retested at 10 weeks of age, for abnormalities in BMD; both wild-type (WT) and mutant mice were tested thereafter at ages as indicated.

FAXITRON ANALYSIS

A high-resolution digital X-ray was taken at a magnification factor of 1.0 at 26 kVp using a Faxitron model MX-20 Specimen Radiography System with a digital camera attachment (Faxitron X-ray Corporation, IL) to determine bone structure of 8-week-old mice. The images were captured on the Specimen Imaging program in the format of Digital Imaging and Communications in Medicine (DICOM) files. Analysis of skeletal abnormalities, and femur and tibia lengths were determined from the DICOM files using the eFilm program (Merge Healthcare, Mississauga, ON).

PLASMA BIOCHEMISTRY

Whole blood was extracted from *Phex*^{Jrt}/+ mice and WT littermates through the saphenous vein and centrifuged to extract plasma. The plasma was stored at −20°C until biochemical analysis (Vita-Tech, Ontario, Canada).

HISTOLOGICAL ANALYSIS

The left femur was dissected from 8- to 10-week-old male mice and fixed in 4% paraformaldehyde for 24 h. Following serial dehydration through from 70% to 100% ethanol, bone was infiltrated and imbedded in methylmethacrylate using the osteo-bed (Polysciences) at 35°C. Coronal sections (5 μm) were taken using a Leica Polycut S through the distal femur and stained with Masson's trichrome [Carson, 1997].

RNA ISOLATION FROM BONE

Three male *Phex*^{Jrt}/Y mice and three WT mice at 32 weeks of age were killed by cervical dislocation. Both right and left femurs and tibiae were isolated from the animals and cleared of associated muscle and connective tissue. The bones were snap frozen in liquid nitrogen and subsequently crushed using a mortar and pestle. RNA was isolated from these samples using Tri reagent (Bioshop) according to the manufacturer's protocol.

REAL-TIME PCR

First-strand cDNA was synthesized from total bone RNA using random hexamers and Superscript III (Invitrogen) according to the supplier's instructions. Quantitative PCR reactions were performed with iQ SYBR Green Supermix using primers for *Phex* (forward primer 5′-GAAAGGGGACCAACCGAGG-3′; reverse primer 5′-AACTTAGGAGACCTTGACTCACT-3′ with product spanning exons 1 and 2), *Fgf23* (forward primer 5′-TGGGCACTGCTAGAGCCTAT-3′; reverse primer 5′-TGGCTCCTGTTATCACCACA-3′), *Opn* (forward primer 5′-AGCAAGAAACTCTTCCAAGCAA-3′; reverse primer 5′-GTGAGATTCGTCAGATTCATCCG-3′), *Mepe* (forward primer 5′-GTCTGTTGGACTGCTCCTCTT-3′; reverse primer 5′-CACCGTGGGATCAGGATACA-3′), *Dmp-1* (forward primer 5′-CATTCTCCTTGTGTTCCTTTGGG-3′; reverse primer 5′-TGTGGTCACTATTTGCCTGTC-3′), *Bsp* (forward primer 5′-CAGGGAGGCAGTGACTCTTC-3′; reverse primer 5′-AGTGTGGAAAGTGTGGCGTT-3′), *Ocn* (forward primer 5′-CTGACCTCACAGATGCCAAGC-3′; reverse primer 5′-TGGTCTGATAGCTCGTCACAAG-3′) and *Sost* (forward primer 5′-TTCAGGAATGATGCCACAGA-3′; reverse primer 5′-GTCAGGAAGCGGGTGTAGTG-3′). Transcript levels were normalized to that of ribosomal protein L32 (forward primer 5′-CACAATGTCAAGGAGCTGGAAGT-3′; reverse primer 5′-TCTACAATGGCTTTTCGGTTCT-3′). The following cycling conditions were used for the reactions in the MyIQ (BioRad): 3-min denaturation and activation step at 95°C, 40 cycles of 10-s annealing and extension at 59°C and denaturation for 30 s at 95°C. Raw data were exported to PCR miner [Zhao and Fernald, 2005] for analysis.

IMMUNOBLOTTING ANALYSIS

Femurs were homogenized in RIPA buffer containing protease inhibitors (Complete Protease Inhibitor Cocktail Tablet, Roche Diagnostics, Indianapolis, IN). Forty μg of homogenates were mixed with Laemmli sample buffer and loaded onto 10% Tris–HCl precast gels (Bio-Rad Laboratories, Hercules, CA). After transfer to PVDF membrane, membranes were blocked with 5% blotto and incubated with anti-PHEX antibody (kindly provided by Dr. Philippe Crine and Dr. Thomas Loisel, Enobia Pharma, Montreal, Canada), and anti-β-actin followed by HRP-conjugated mouse antibody. Detection was done with Amersham ECL Western Blotting Detection Reagents (GE Healthcare, Piscataway, NJ).

BONE MARROW STROMAL CELL ISOLATION AND CULTURE

Three *Phex*^{Jrt}/+ mice and three WT mice at 5 months of age were killed by cervical dislocation. Bone marrow was recovered from the resected femurs and tibiae by centrifugation, resuspended in basal culture medium (α-MEM supplemented with 15% heat-inactivated fetal bovine serum and antibiotics (100 U/ml penicillin G, 50 μg/ml gentamycin sulfate, and 0.3 μg/ml amphotericin B), counted and plated at densities of 0.5 or 1×10^6 cells/ml in 35 mm culture dishes in the basal culture medium for 72 h at 37°C in humidified air with 5% CO_2. The medium was then changed to osteoblast differentiation medium (α-MEM supplemented with 10% FBS, antibiotics as above 50 μg/ml ascorbic acid, and 10 mM β-glycerophosphate) and the cells were maintained in culture until mineralized nodules formed (21 days), with medium changes every 2–3 days. At the endpoint, five culture plates from each animal were stained for alkaline phosphatase (ALP) and with Von Kossa stain, and the remaining plates were used for RNA and protein isolation. Stained plates were photographed using a digital camera, and the resulting images were used to quantify ALP and/or Von Kossa positive colonies with the aid of the ImageJ program (Research Services Branch, National Institute of Mental Health, Bethesda, MD).

For the calcium deposition assay, cells were recovered and cultured as above, but excluding β-glycerophosphate in the differentiation medium for 14–17 days. β-Glycerophosphate was then added for 1, 2, or 3 days; at each time point, cells were washed with PBS, and the calcium deposits extracted by overnight incubation with 0.6 N HCl. Calcium concentration was determined using a colorimetric calcium determination kit (Sigma 587-A kit).

STATISTICAL ANALYSIS

Data are expressed as the mean ± standard deviation or standard error of the mean as indicated, followed by analysis using GraphPad Prism 4 with two-sample, unpaired *t*-tests with a confidence interval of 95% unless otherwise stated. A *P*-value of <0.05 was considered statistically significant.

RESULTS

GENERATION AND CHARACTERIZATION OF THE *Phex*^{Jrt} MOUSE LINE

A 129;B6F1 female from the ENU mutagenesis screen was identified by its low BMD, smaller body size, and shortened tail; this mouse was bred with WT C57BL/6J males to produce several generations of mice on the C57BL/6J background, of which all the affected mice had the same traits. Despite the fully penetrant physical abnormalities of the affected mice, their life span and fertility remain equivalent to that of WT littermates. Both hemizygous male (*Phex*^{Jrt}/Y) and heterozygous female (*Phex*^{Jrt}/+) mice are affected by the mutation, but abnormalities are more severe in male mice, and affected males produce only affected females. Genetic mapping of affected mice confirmed that the mutation is located on the X chromosome within a 33.7-Mb interval containing *Phex* (Fig. 1A). Sequencing of *Phex* identified an adenine to thymine replacement (Fig. 1B) in the fourth base pair of exon 14 which introduces a stop codon at amino acid 496 (allele named *Phex*^{Jrt}). The predicted protein product is a truncated form of the Phex protein missing part of the extracellular domain including the zinc-binding motif and four conserved cysteine residues (Fig. 1A). In bone from *Phex*^{Jrt}/Y males, mutant Phex mRNA is expressed but is markedly reduced (~20%) compared to that of WT (Fig. 1C) whereas PHEX is not detectable by immunoblot analysis (Fig. 1D). PHEX is also absent in bone from homozygous mutant females, but is present in reduced amounts in the heterozygous females.

Consistent with the growth retardation characteristic of XLH, mutant mice have lower body weight—at 8 weeks of age, male *Phex*^{Jrt}/Y mice have a mean weight of 19.2 ± 3.0 g versus the mean WT weight of 24.8 ± 2.1 g ($P<0.001$) and female *Phex*^{Jrt}/+ mice have a mean weight of 16.1 ± 1.9 g versus the mean WT weight of 18.9 ± 1.2 g ($P<0.001$)—and are significantly smaller and shorter (total body length) than their WT littermates at the ages tested (Fig. 2A–C). Faxitron X-ray analysis of *Phex*^{Jrt}/+ mice at 8 weeks of age revealed many skeletal aberrations, manifested not only by shorter bones throughout the skeleton including the tibiae and femurs (Fig. 2D) and vertebrae (note the small tail vertebrae), but also by abnormal curvature of pelvic and long bones consistent with

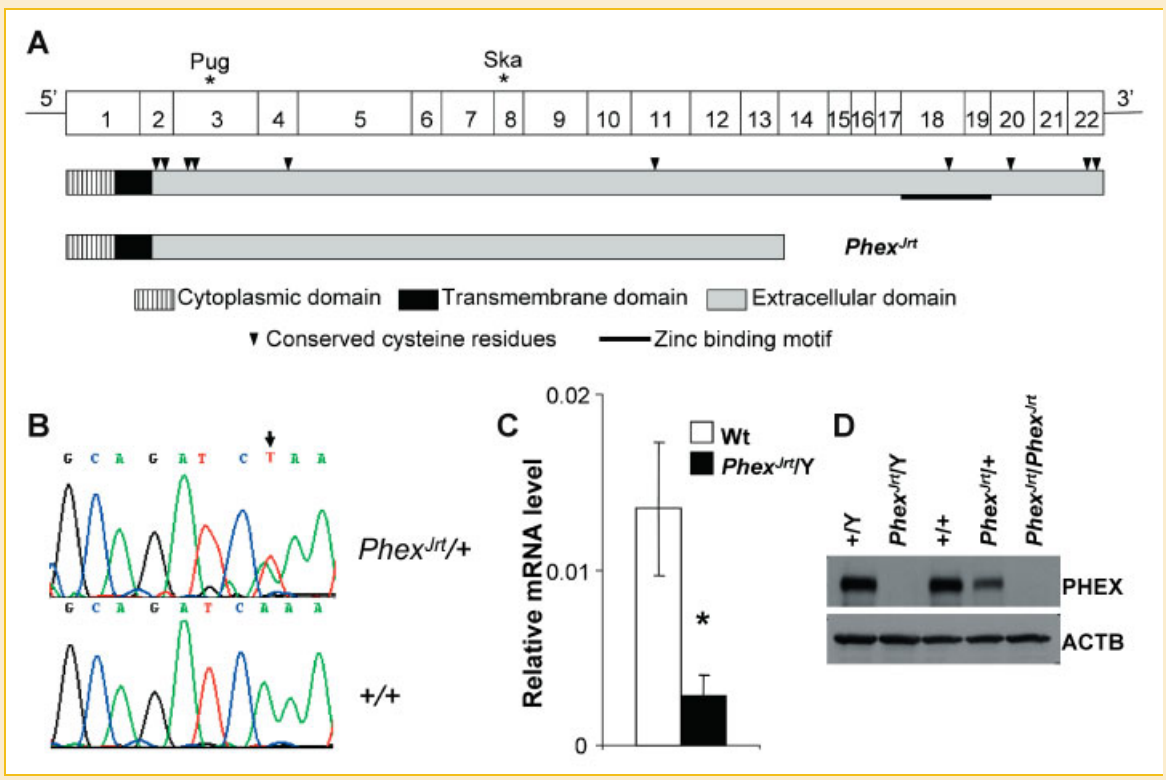

Fig. 1. *Phex*^{Jrt} mutation and effect on Phex mRNA and protein expression levels. A: Schematic diagram of Phex mRNA and protein domains (modified from [Tenenhouse, 1999]). The *Phex*^{Jrt} protein, if expressed, is predicted to be a truncated protein missing part of its extracellular domain. The location of *Pug* [Xiong et al., 2008] and *Ska* [Carpinelli et al., 2002] mutations are shown in above schematic for Phex mRNA. B: Forward strand traces of the Phex genomic sequence spanning the mutation in *Phex*^{Jrt}/+ (top) and the corresponding site in a WT littermate (bottom). C: Phex mRNA levels of mineralized stromal cultures from male (32-week old), *Phex*^{Jrt}/Y (filled bars) and age-matched WT mice (empty bars). *$P<0.05$, unpaired *t*-test. D: Immunoblot analysis of protein from femurs of mutant male hemizygous (*Phex*^{Jrt}/Y), female heterozygous (*Phex*^{Jrt}/+) and homozygous (*Phex*^{Jrt}/*Phex*^{Jrt}) mice, and WT littermate using anti-PHEX antibody (top) and anti-β-actin antibody (bottom).

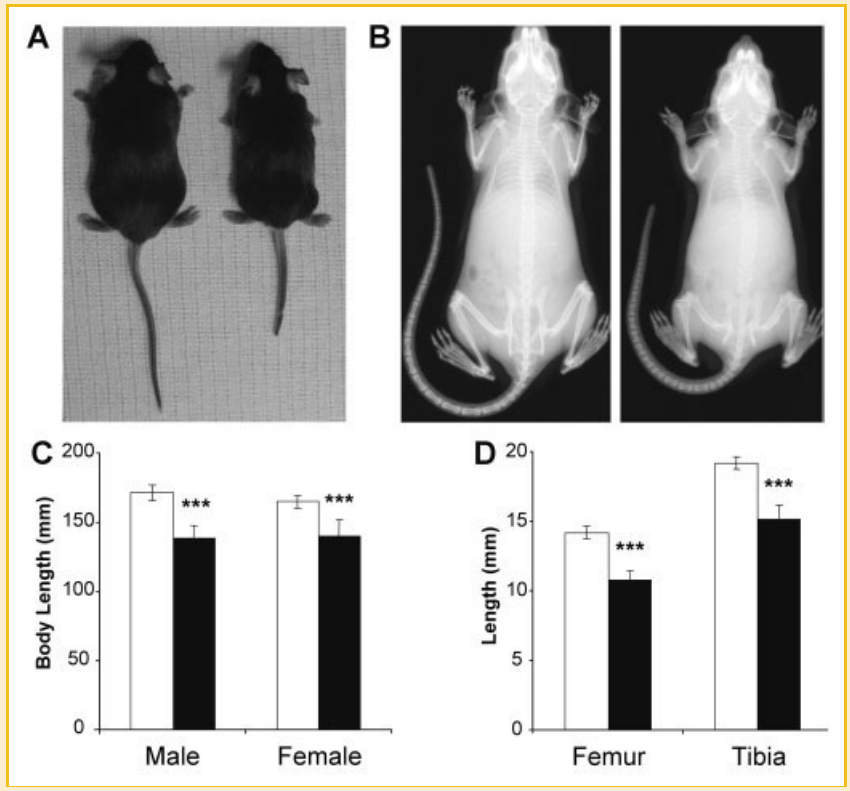

Fig. 2. Whole animal and skeletal characteristics of *Phex*^{Jrt} versus WT mice. A: *Phex*^{Jrt}/Y (right) mice are smaller and have shorter tails than their WT littermates (left). Shown are 12-week-old mice. B: Faxitron X-ray images of WT (left) and *Phex*^{Jrt}/+ (right) mice at 8 weeks of age. C: Body lengths of age-matched (10-week old), sex-matched mutant (filled bars) and WT (empty bars) mice. D: Tibial and femoral lengths of male *Phex*^{Jrt}/Y mice (filled bars) compared to age-matched (8-week old) sex-matched WT mice (empty bars).

rickets (Fig. 2B). There was also marked enlargement of all joints in the *Phex*^{Jrt}/+ mice (Fig. 2B).

Phex^{Jrt} mice have significantly lower BMC (Fig. 3A) and BMD (Fig. 3B). During resection, it was observed that long bones from mutant mice were easily deformed, a sign they might be severely undermineralized. Histological analysis of undecalcified bone samples confirmed that *Phex*^{Jrt}/Y (Fig. 3C) mice have severe osteomalacia. Osteoid seams were thicker in both the cortical and the nearly absent metaphyseal trabecular bone. In addition to the osteomalacia, the femoral bone displayed features typical of rickets with a strikingly enlarged growth plate and comparatively narrow shaft. The femoral growth plate in Phex bone was abnormal in both thickness, with an expanded proliferative zone and organization. The unusual location of hypertrophic cells within the growth plate in sections suggests that irregular organization occurs not only along the proximal–distal axis, but along the lateral axis as well. Lastly, non-calcified cartilage persists adjacent to the growth plate.

Since one of the hallmarks of XLH is hypophosphatemia, we analyzed serum parameters for phosphorus as well as for calcium and ALP levels which are also known to be affected in the bone disease. Analysis of serum parameters showed that all three parameters were affected: phosphate levels were significantly lower, calcium levels slightly, but significantly lower and ALP levels were significantly elevated in mutant hemizygous males (*Phex*^{Jrt}/Y) and heterozygous females (*Phex*^{Jrt}/+) versus gender-matched WT mice (Table I). No significant differences were found in serum parameters between hemizygous males and heterozygous females.

EFFECT OF PHEX MUTATION ON *Fgf23*, *Bsp*, *Ocn*, *Opn*, *Mepe*, AND *Sost* mRNA EXPRESSION

Since FGF23, a suspected phosphaturic factor in XLH, is increased in serum from XLH and the *Hyp* mouse, we examined the effect the *Phex*^{Jrt} mutation has on the expression levels of *Fgf23*. In *Phex*^{Jrt}/Y cortical bone, *Fgf23* mRNA expression was significantly increased (Fig. 4A), consistent with the previously reported higher levels of FGF23 in mutant mouse serum [Ichikawa et al., 2012].

Hyp bone has been shown to have altered levels of matrix proteins including some that belong to the SIBLING family, which are known positive and negative regulators of mineralization [Carpenter and Gundberg, 1996; Argiro et al., 2001; Miao et al., 2001; Atkins et al., 2011]. The levels of *Bsp*, *Mepe*, and *Ocn* were increased in the *Phex*^{Jrt}/Y cortical bone whereas *Sost* expression was unaffected (Fig. 4B). In heterozygous Phex^{Jrt}/+ females, these same genes were unaffected (data not shown).

Phex^{Jrt}/Y OSTEOBLASTS DIFFERENTIATE AND MINERALIZE DEPOSITED OSTEOID IN VITRO

Since previous reports have shown that there is an intrinsic defect in the osteoblasts of *Hyp* mice [Xiao et al., 1998; Liu et al., 2002], stromal cells from *Phex*^{Jrt}/Y mice were tested for their ability to

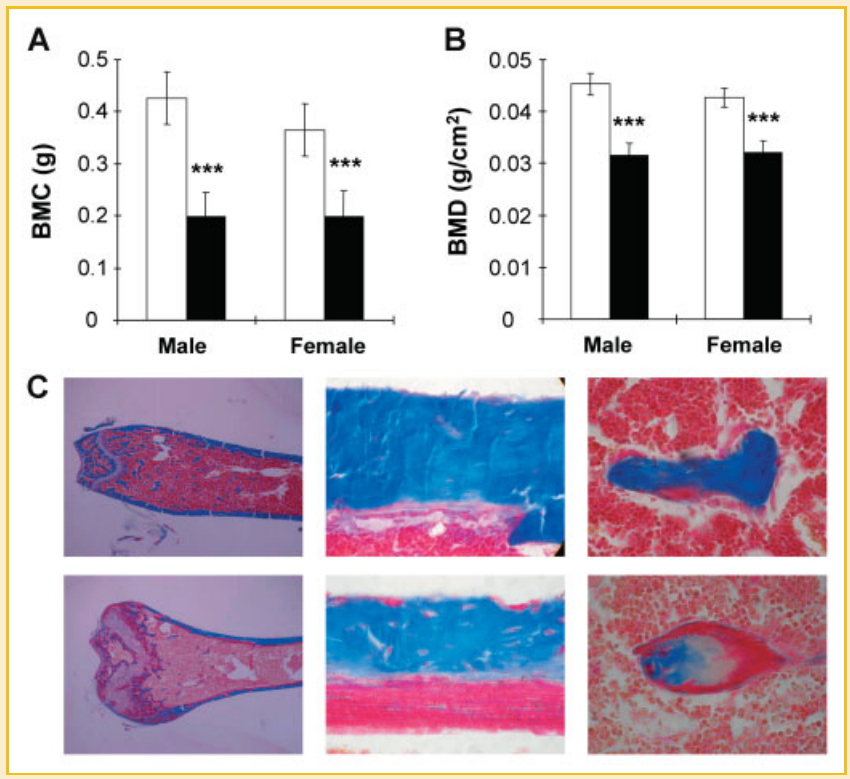

Fig. 3. Bone parameters and histology of *Phex*^{Jrt} mice. A: Bone mineral content and (B) bone mineral density for 8-week-old male (*Phex*^{Jrt}/Y) and female (*Phex*^{Jrt}/+) mice (filled bars) and their age- and sex-matched WT (empty bars) littermates. Error bars represent standard deviation. $^{***}P < 0.001$ unpaired *t*-test. Histology of mid-coronal plastic sections from the distal femur of WT (top) and *Phex*^{Jrt}/Y mice (bottom) stained with (C) Masson trichrome showing osteoid (red) and extent of mineralization (blue) of distal femur (left), endosteum (center), and trabeculae (right) in *Phex*^{Jrt}/Y bone (bottom) compared with control bone (WT). Mice were 8 weeks of age.

differentiate in vitro. Cells from *Phex*^{Jrt}/Y and WT mice were grown in the presence of differentiation medium and stopped by fixation when mineralized colonies were evident in cells from WT mice. *Phex*^{Jrt}/Y cells produced similar numbers of colony forming units-ALP (CFU-ALP) and mineralized bone colonies (CFU-O) to WT cells (Fig. 5A,B).

To further determine whether there is a cell-autonomous mineralization defect in the *Phex*^{Jrt}/Y osteoblasts, stromal cultures were grown in the presence of ascorbic acid until matrix deposition was evident in WT cultures after which β-glycerophosphate was added to all the cultures. No difference was detected between *Phex*^{Jrt}/Y and WT osteoblasts in the amount of calcium deposited into the matrix at 24-, 36-, and 48-h after β-glycerophosphate addition (Fig. 5C).

DISCUSSION

The *Phex*^{Jrt} mutation described in this report is a new ENU-generated point mutation of adenine to thymine in exon 14 which introduces a premature stop codon. *Phex* expression levels are significantly reduced in the mutant carriers and the protein is undetectable in homozygous *Phex*^{Jrt} females and hemizygous males. Since the mutation is unlikely to affect gene promoter activity, non sense-mediated mRNA decay of the transcript is likely the key to the low steady-state levels of *Phex*. Consistent with the decrease in PHEX expression, *Phex*^{Jrt}/Y and *Phex*^{Jrt}/+ mice manifest growth retardation, shortened hind limbs and tail, osteomalacia, and hypophosphatemia with mild hypocalcemia, and elevated serum ALP. Other common features of XLH, including deformities in the epiphyseal

TABLE I. Serum Chemical and Biochemical Analysis

	Mean value ± SEM (n)			
	WT male	Phex^{Jrt}/Y	WT female	Phex^{Jrt}/+
Alkaline phosphatase (U/L)	125 ± 17 (4)	394 ± 48** (5)	162 ± 6 (8)	402 ± 32** (7)
Phosphorus (mmol/L)	1.9 ± 0.0 (3)	1.1 ± 0.2* (3)	1.7 ± 0.1 (6)	0.82 ± 0.06** (5)
Calcium (mmol/L)	2.34 ± 0.03 (3)	2.16 ± 0.02* (3)	2.34 ± 0.03 (5)	2.19 ± 0.01* (4)

$^{*}P$-value < 0.01 between gender-matched littermates.
$^{**}P$-value < 0.001 between gender-matched littermates.

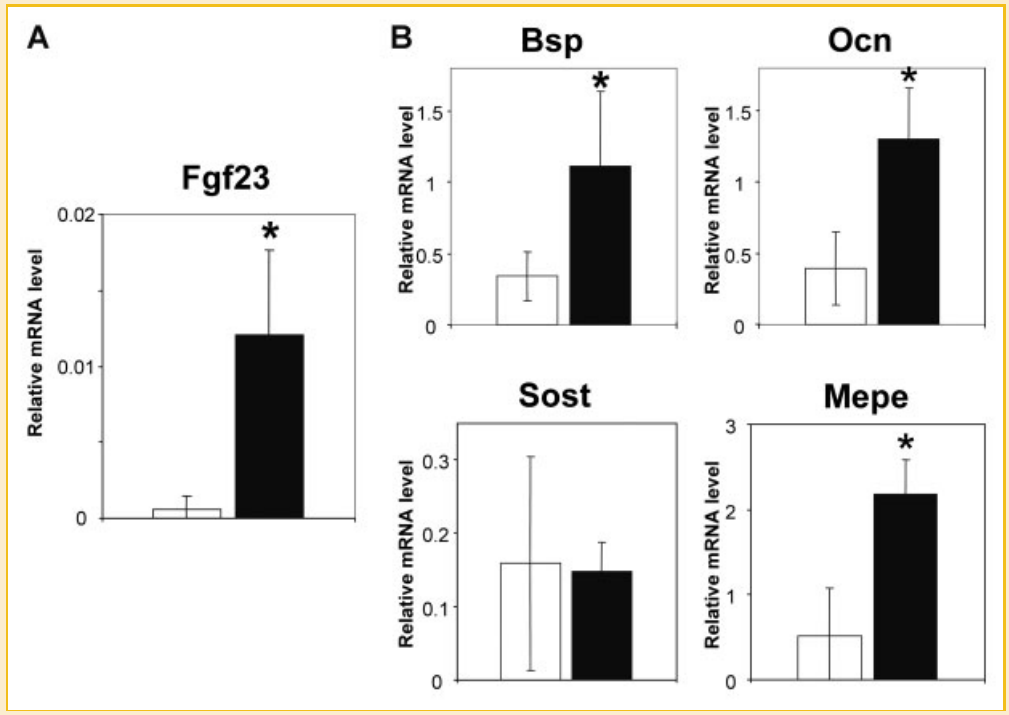

Fig. 4. mRNA expression levels of bone markers in combined femoral and tibial cortical bone. A: Fgf23 mRNA levels and (B) expression levels for *Ocn*, SIBLING proteins *Bsp*, and *Mepe* as well as that for *Sost*. Samples were taken from male age-matched (29-week old) $Phex^{Jrt}$/Y (filled bars) and WT mice (empty bars). Error bars represent standard deviation. $^{*}P < 0.05$, unpaired *t*-test.

growth plate and marked enlargement of all joints thought to be secondary to rickets [Drezner, 2000], were also seen.

Several earlier studies report the existence of an intrinsic defect in *Hyp* osteoblasts. Immortalized osteoblast cells derived from calvaria of *Hyp* mice and cultured in differentiation medium are unable to mineralize [Xiao et al., 1998; Liu et al., 2002] and the response of primary *Hyp* calvarial osteoblasts to $1,25(OH)_2D_3$ appears to be sensitive to phosphate concentrations unlike that of normal osteoblasts [Yamamoto et al., 1992]. Still others have found abnormalities in OPN phosphorylation [Rifas et al., 1997] and elevated serum levels of OCN in *Hyp* mice further supporting an osteoblast defect in the *Hyp* mutant [Gundberg et al., 1992]. However, in spite of both *Hyp* [Ruchon et al., 2000; Bai et al., 2002; Thompson et al., 2002] and $Phex^{Jrt}$ male mice having no detectable PHEX in bone tissue, $Phex^{Jrt}$/Y osteoblasts have no measurable temporal or endpoint differentiation or mineralization defects in vitro and furthermore expression of *Sost* is unaffected. The reasons for the discrepancy between our results and those from *Hyp* mice are not known, although the source of osteoblasts tested, calvaria versus bone marrow, the use of clonal immortalized cell lines as opposed to primary cultures, or the intergenic deletion and its incompletely characterized effect on the downstream spermidine/spermine *N*1-acetyl transferase (*Sat*) gene [Sabbagh et al., 2002] may be factors. Interestingly, BMSC from *Hyp* mice grown in differentiation medium do mineralize, though less than that from WT mice [Martin et al., 2011].

Several compelling lines of evidence point to a role for FGF23 in mediating the kidney effects of various *PHEX*/*Phex* mutations in XLH. Directly injected recombinant or transgenically overexpressed FGF23 causes phosphaturia and hypophosphatemia [Shimada et al., 2001; Bai et al., 2004], mutations near the FGF23 cleavage site allowing it to resist inactivating protease action are responsible for autosomal dominant hypophosphatemic rickets (ADHR) [White et al., 2001; Bai et al., 2003] and FGF23 is upregulated in *Hyp* mouse [Liu et al., 2006]. We have found that both Fgf23 gene and protein expression are highly increased in the $Phex^{Jrt}$/Y mutant mouse as in the *Hyp* mouse, a finding consistent with the observed phosphaturia.

While FGF23 appears to mediate mineralization indirectly through its effect on serum phosphorus levels via kidney function and overexpression of FGF23 has been shown to directly inhibit mineralization in rat calvarial culture [Wang et al., 2008], growing evidence supports the role of another protein, MEPE, in bone mineralization, specifically its ASARM peptide cleavage product as MEPE-ASARM peptides inhibit mineralization both in vivo and in vitro [Rowe et al., 2004]. Expression of *Mepe* has been shown to be elevated in *Hyp* osteoblasts [Argiro et al., 2001] and is similarly elevated in $Phex^{Jrt}$/Y bone.

Our model of XLH is distinct from the well-studied *Hyp* mouse although they share many similarities; both have osteomalacic bone, hypophosphatemia, abnormal serum levels of calcium and ALP, growth plate defects, and increased FGF23 levels. Unlike *Hyp* osteoblasts, $Phex^{Jrt}$/Y osteoblasts appear not to have an intrinsic mineralization defect and more strikingly, the expression of *Sost*, whose protein product is increased in *Hyp* and has been hypothesized to play a role in the mineralization defect in that XLH model [Atkins et al., 2011], is unaffected in both male and

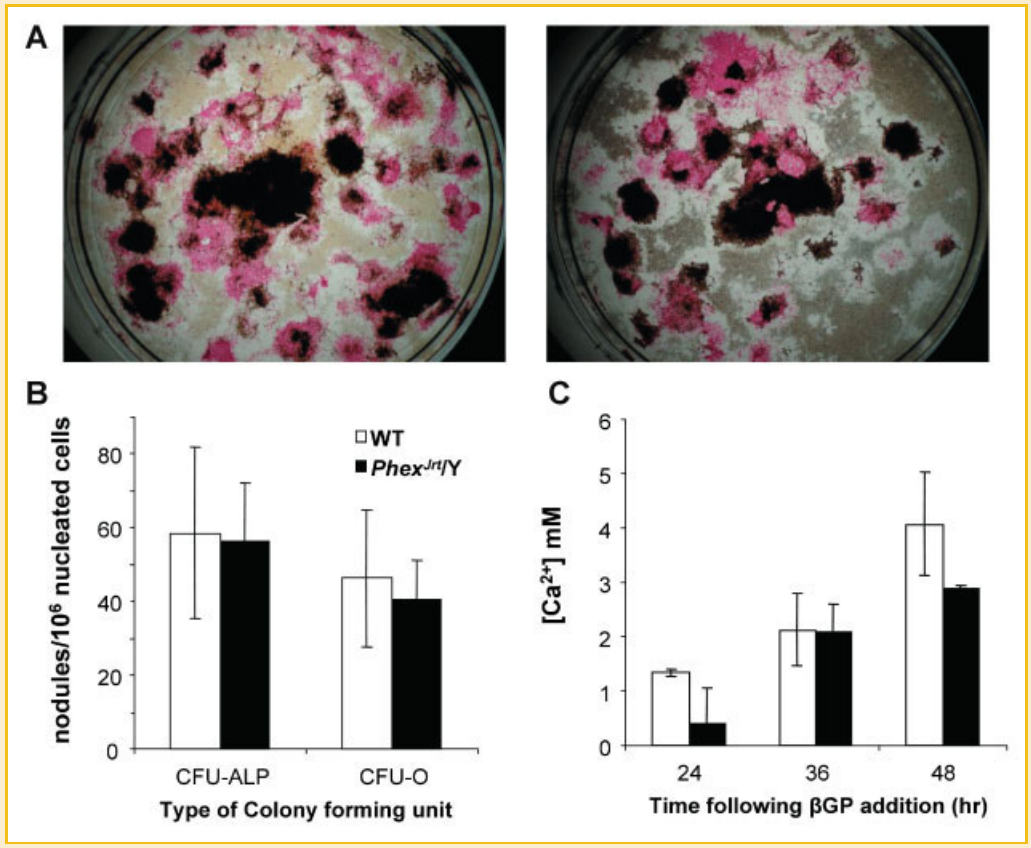

Fig. 5. *Phex*^{Jrt} mutation and effect on bone marrow osteoprogenitor number and ability to form mineralized nodules. A: Bone marrow cultures from WT (left) and *Phex*^{Jrt}/Y mice (right) were stained on day 19 for alkaline phosphatase activity and mineralization (Von Kossa). B: Number of osteoprogenitors and (C) calcium deposition were unaffected in culture from *Phex*^{Jrt}/Y mice (filled bars) when compared with that from WT cultures (empty bars). Error bars represent standard deviation. $P > 0.05$ in a one-way ANOVA, Tukey Kramer multiple comparison tests.

female *Phex*^{Jrt} mice. These traits may provide a useful new tool for teasing out the multiple functions of PHEX. Finally, it will be a useful addition to the group of existing mouse models for the testing of new therapeutics for osteomalacia.

ACKNOWLEDGMENTS

We thank other members (Igor Vukobradovic, Zorana Berberovic, Lois Kelsey, Irina Voronina, and Nora Tsao) of the Centre for Modeling Human Disease (CMHD) for their support, Lily Morikawa and staff at the CMHD Pathology Core for their histological expertise, Dr. Dean Percy for his help, Feryal Sarraf at the Faculty of Dentistry for her technical expertise with histology, Dr. Michael J. Econs of the Department of Medicine, Indiana University School of Medicine for reading the article and helpful comments, and other members (Dr. Ralph Zirngibl, Tanya Zappitelli, Marco Cardelli, Usha Bhargava) of the Aubin lab for their support and help. This research was supported by Genome Canada and the Ontario Genomic Institute and by the Canadian Institutes of Health Research [CIHR (MOP 69198 to J.E.A., a Group grant to J.R., J.E.A., S.L.A., and a CIHR distinguished scientist award to J.R.) and operating grant FRN 69198 to J.E.A. and KL2 career development award to S.I. from the Indiana Clinical and Translational Sciences Institute funded in part by the National Institutes of Health grant RR025760.

REFERENCES

Argiro L, Desbarats M, Glorieux FH, Ecarot B. 2001. MEPE, the gene encoding a tumor-secreted protein in oncogenic hypophosphatemic osteomalacia, is expressed in bone. Genomics 74:342–351.

Atkins GJ, Rowe PS, Lim HP, Welldon KJ, Ormsby R, Wijenayaka AR, Zelenchuk L, Evdokiou A, Findlay DM. 2011. Sclerostin is a locally acting regulator of late-osteoblast/pre-osteocyte differentiation and regulates mineralization through a MEPE-ASARM dependent mechanism. J Bone Miner Res 26:1425–1436.

Bai XY, Miao DS, Panda D, Grady S, McKee MD, Goltzman D, Karaplis AC. 2002. Partial rescue of the Hyp phenotype by osteoblast-targeted PHEX (phosphate-regulating gene with homologies to endopeptidases on the X chromosome) expression. Mol Endocrinol 16:2913–2925.

Bai X-Y, Miao D, Goltzman D, Karaplis AC. 2003. The autosomal dominant hypophosphatemic rickets R176Q mutation in fibroblast growth factor 23 resists proteolytic cleavage and enhances in vivo biological potency. J Biol Chem 278:9843–9849.

Bai X, Miao D, Li J, Goltzman D, Karaplis AC. 2004. Transgenic mice overexpressing human fibroblast growth factor 23 (R176Q) delineate a putative role for parathyroid hormone in renal phosphate wasting disorders. Endocrinology 145:5269–5279.

Carpenter TO, Gundberg CM. 1996. Osteocalcin abnormalities in Hyp mice reflect altered genetic expression and are not due to altered clearance, affinity for mineral, or ambient phosphorus levels. Endocrinology 137: 5213–5219.

Carpinelli MR, Wicks IP, Sims NA, O'Donnell K, Hanzinikolas K, Burt R, Foote SJ, Bahlo M, Alexander WS, Hilton DJ. 2002. An ethyl-nitrosourea-induced point mutation in Phex causes exon skipping, X-linked hypophosphatemia, and rickets. Am J Pathol 161:1925–1933.

Carson FL. 1997. Histotechnology: A self-instructional text. Chicago: ASCP Press.

Christie PT, Harding B, Nesbit MA, Whyte MP, Thakker RV. 2001. X-linked hypophosphatemia attributable to pseudoexons of the PHEX gene. J Clin Endocrinol Metab 86:3840–3844.

Drezner MK. 2000. PHEX gene and hypophosphatemia. Kidney Int 57:9–18.

Du L, Desbarats M, Viel J, Glorieux FH, Cawthorn C, Ecarot B. 1996. cDNA cloning of the murine Pex gene implicated in X-linked hypophosphatemia and evidence for expression in bone. Genomics 36:22–28.

Filisetti D, Ostermann G, von Bredow M, Strom T, Filler G, Ehrich J, Pannetier S, Garnier JM, Rowe P, Francis F, Julienne A, Hanauer A, Econs MJ, Oudet C. 1999. Non-random distribution of mutations in the PHEX gene, and under-detected missense mutations at non-conserved residues. Eur J Hum Genet 7:615–619.

Francis F, Hennig S, Korn B, Reinhardt R, Dejong P, Poustka A, Lehrach H, Rowe PSN, Goulding JN, Summerfield T, Mountford R, Read AP, Popowska E, Pronicka E, Davies KE, Oriordan JLH, Econs MJ, Nesbitt T, Drezner MK, Oudet C, Pannetier S, Hanauer A, Strom TM, Meindl A, Lorenz B, Cagnoli M, Mohnike KL, Murken J, Meitinger T. 1995. A gene (Pex) with homologies to endopeptidases is mutated in patients with X-linked hypophosphatemic rickets. Nat Genet 11:130–136.

Francis F, Strom TM, Hennig S, Boddrich A, Lorenz B, Brandau O, Mohnike KL, Cagnoli M, Steffens C, Klages S, Borzym K, Pohl T, Oudet C, Econs MJ, Rowe PSN, Reinhardt R, Meitinger T, Lehrach H. 1997. Genomic organization of the human PEX gene mutated in X-linked dominant hypophosphatemic rickets. Genome Res 7:573–585.

Gundberg CM, Clough ME, Carpenter TO. 1992. Development and validation of a radioimmunoassay for mouse osteocalcin—Paradoxical response in the Hyp mouse. Endocrinology 130:1909–1915.

Holm IA, Huang X, Kunkel LM. 1997. Mutational analysis of the PEX gene in patients with X-linked hypophosphatemic rickets. Am J Hum Genet 60: 790–797.

Holm IA, Nelson AE, Robinson BG, Mason RS, Marsh DJ, Cowell CT, Carpenter TO. 2001. Mutational analysis and genotype–phenotype correlation of the PHEX gene in X-linked hypophosphatemic rickets. J Clin Endocrinol Metab 86:3889–3899.

Ichikawa S, Traxler EA, Estwick SA, Curry LR, Johnson ML, Sorenson AH, Imel EA, Econs MJ. 2008. Mutational survey of the PHEX gene in patients with X-linked hypophosphatemic rickets. Bone 43:663–666.

Ichikawa S, Austin AM, Gray AK, Econs MJ. 2012. A Phex mutation in a murine model of X-linked hypophosphatemia alters phosphate responsiveness of bone cells. J Bone Miner Res 27:453–460.

Liu S, Guo R, Tu Q, Quarles LD. 2002. Overexpression of Phex in osteoblasts fails to rescue the Hyp mouse phenotype. J Biol Chem 277:3686–3697.

Liu S, Zhou J, Tang W, Jiang X, Rowe DW, Quarles LD. 2006. Pathogenic role of Fgf23 in Hyp mice. Am J Physiol Endocrinol Metab 291:E38–E49.

Liu SG, Gupta A, Quarles LD. 2007. Emerging role of fibroblast growth factor 23 in a bone–kidney axis regulating systemic phosphate homeostasis and extracellular matrix mineralization. Curr Opin Nephrol Hypertens 16:329–335.

Lobaugh B, Burch WJ, Drezner M. 1984. Abnormalities of vitamin D metabolism and action in the vitamin D resistant rachitic and osteomalacic diseases. In: Kumar R, editor. Vitamin D: Basic and clinical aspects. Boston: Martinus Nijhoff. pp 665–720.

Lorenz-Depiereux B, Guido VE, Johnson KR, Zheng QY, Gagnon LH, Bauschatz JD, Davisson MT, Washburn LL, Donahue LR, Strom TM, Eicher EM. 2004. New intragenic deletions in the Phex gene clarify X-linked hypophosphatemia-related abnormalities in mice. Mamm Genome 15: 151–161.

Martin A, Liu S, David V, Li H, Karydis A, Feng JQ, Quarles LD. 2011. Bone proteins PHEX and DMP1 regulate fibroblastic growth factor Fgf23 expression in osteocytes through a common pathway involving FGF receptor (FGFR) signaling. FASEB J 25:2551–2562.

Miao D, Bai X, Panda D, McKee MD, Karaplis AC, Goltzman D. 2001. Osteomalacia in Hyp mice is associated with abnormal Phex expression and with altered bone matrix protein expression and deposition. Endocrinology 142:926–939.

Moriyama K, Hanai A, Mekada K, Yoshiki A, Ogiwara K, Kimura A, Takahashi T. 2011. Kbus/Idr, a mutant mouse strain with skeletal abnormalities and hypophosphatemia: Identification as an allele of 'Hyp'. J Biomed Sci 18:60.

Rasmussen H, Tenenhouse H. 1995. Mendelian hypophosphatemias. In: Scriver C, Beaudet A, Sly W, Valle D, editors. The metabolic and molecular basis of inherited disease. New York: McGraw Hill. pp 3717–3745.

Rifas L, Cheng SL, Halstead LR, Gupta A, Hruska KA, Avioli LV. 1997. Skeletal casein kinase activity defect in the HYP mouse. Calcif Tissue Int 61:256–259.

Rowe PSN, Oudet CL, Francis F, Sinding C, Pannetier S, Econs MJ, Strom TM, Meitinger T, Garabedian M, David A, Macher MA, Questiaux E, Popowska E, Pronicka E, Read AP, Mokrzycki A, Glorieux FH, Drezner MK, Hanauer A, Lehrach H, Goulding JN, Oriordan JLH. 1997. Distribution of mutations in the PEX gene in families with X-linked hypophosphataemic rickets (HYP). Hum Mol Genet 6:539–549.

Rowe PSN, Kumagai Y, Gutierrez G, Garrett IR, Blacher R, Rosen D, Cundy J, Navvab S, Chen D, Drezner MK, Quarles LD, Mundy GR. 2004. MEPE has the properties of an osteoblastic phosphatonin and minhibin. Bone 34:303–319.

Ruchon AF, Tenenhouse HS, Marcinkiewicz M, Siegfried G, Aubin JE, Desgroseillers L, Crine P, Boileau G. 2000. Developmental expression and tissue distribution of Phex protein: Effect of the Hyp mutation and relationship to bone markers. J Bone Miner Res 15:1440–1450.

Sabbagh Y, Jones AO, Tenenhouse HS. 2000. PHEXdb, a locus-specific database for mutations causing X-linked hypophosphatemia. Hum Mutat 16:1–6.

Sabbagh Y, Gauthier C, Tenenhouse HS. 2002. The X chromosome deletion in Hyp mice extends into the intergenic region but does not include the Sat gene downstream from Phex. Cytogenet Genome Res 99:344–349.

Sabbagh Y, Boileau G, Campos M, Carmona AK, Tenenhouse HS. 2003. Structure and function of disease-causing missense mutations in the PHEX gene. J Clin Endocrinol Metab 88:2213–2222.

Shimada T, Mizutani S, Muto T, Yoneya T, Hino R, Takeda S, Takeuchi Y, Fujita T, Fukumoto S, Yamashita T. 2001. Cloning and characterization of FGF23 as a causative factor of tumor-induced osteomalacia. Proc Natl Acad Sci USA 98:6500–6505.

Strom TM, Juppner H. 2008. PHEX, FGF23, DMP1 and beyond. Curr Opin Nephrol Hypertens 17:357–362.

Strom TM, Francis F, Lorenz B, Boddrich A, Econs MJ, Lehrach H, Meitinger T. 1997. Pex gene deletions in Gy and Hyp mice provide mouse models for X-linked hypophosphatemia. Hum Mol Genet 6:165–171.

Tenenhouse HS. 1999. X-linked hypophosphataemia: A homologous disorder in humans and mice. Nephrol Dial Transplant 14:333–341.

Thompson DL, Sabbagh Y, Tenenhouse HS, Roche PC, Drezner MK, Salisbury JL, Grande JP, Poeschla EM, Kumar R. 2002. Ontogeny of Phex/PHEX protein expression in mouse embryo and subcellular localization in osteoblasts. J Bone Miner Res 17:311–320.

Turner AJ, Tanzawa K. 1997. Mammalian membrane metallopeptidases: NEP, ECE, KELL, and PEX. FASEB J 11:355–364.

Wang H, Yoshiko Y, Yamamoto R, Minamizaki T, Kozai K, Tanne K, Aubin JE, Maeda N. 2008. Overexpression of fibroblast growth factor 23 suppresses osteoblast differentiation and matrix mineralization in vitro. J Bone Miner Res 23:939–948.

White KE, Carn G, Lorenz-Depiereux B, Benet-Pages A, Strom TM, Econs MJ. 2001. Autosomal-dominant hypophosphatemic rickets (ADHR) mutations stabilize FGF-23. Kidney Int 60:2079–2086.

Xiao ZS, Crenshaw M, Guo R, Nesbitt T, Drezner MK, Quarles LD. 1998. Intrinsic mineralization defect in Hyp mouse osteoblasts. Am J Physiol 275:E700–E708.

Xiong XW, Qi X, Ge XM, Gu PY, Zhao J, Zhao QS, Gao X. 2008. A novel Phex mutation with defective glycosylation causes hypophosphatemia and rickets in mice. J Biomed Sci 15:47–59.

Yamamoto T, Ecarot B, Glorieux FH. 1992. Abnormal response of osteoblasts from Hyp mice to 1,25-dihydroxyvitamin D3. Bone 13:209–215.

Yuan B, Takaiwa M, Clemens TL, Feng JQ, Kumar R, Rowe PS, Xie Y, Drezner MK. 2008. Aberrant Phex function in osteoblasts and osteocytes alone underlies murine X-linked hypophosphatemia. J Clin Investig 118:722–734.

Zhao S, Fernald RD. 2005. Comprehensive algorithm for quantitative real-time polymerase chain reaction. J Comput Biol 12:1047–1064.